Vision Research

Attentional control over either of the two competing percepts of ambiguous stimuli revealed by a two-parameter analysis: Means do not make the difference

R. van Ee *, A.J. Noest, J.W. Brascamp, A.V. van den Berg

Utrecht University, Helmholtz Institute, The Netherlands

Abstract

We studied distributions of perceptual rivalry reversals, as defined by the two fitted parameters of the Gamma distribution. We did so for a variety of bi-stable stimuli and voluntary control exertion tasks. Subjects' distributions differed from one another for a particular stimulus and control task in a systematic way that reflects a constraint on the describing parameters. We found a variety of two-parameter effects, the most important one being that distributions of subjects differ from one another in the same systematic way across different stimuli and control tasks (i.e., a fast switcher remains fast across all conditions in a parameter-specified way). The cardinal component of subject-dependent variation was not the conventionally used mean reversal rate, but a component that was oriented—for all stimuli and tasks—roughly perpendicular to the mean rate. For the Necker cube, we performed additional experiments employing specific variations in control exertion, suggesting that subjects have to a considerable extent independent control over the reversal rate of either of the two competing percepts.
© 2006 Elsevier Ltd. All rights reserved.

1. Introduction

Observers are able to influence the duration of a percept when they experience perceptual bi-stability as a result of viewing ambiguous images (review in Leopold & Logothetis, 1999). The extent to which this voluntary control influences the reversals in perceptual bi-stability can be quantified (e.g., Hol, Koene, & van Ee, 2003; Lack, 1978; Meng & Tong, 2004; Peterson & Hochberg, 1983; Suzuki & Peterson, 2000; Toppino, 2003; van Ee, van Dam, & Brouwer, 2005) to study voluntary control as a biological phenomenon.

The mechanism(s) of bi-stable perception are reflected in its dynamics and, therefore, a thorough systematic charac-

terization of the dynamics is important for understanding these mechanisms. It is generally agreed that the stochastic variation around the mean perceptual reversal rate (i.e., the distribution) is a characteristic feature of rivalry. In previous work the nature of these distributions has been studied (Borsellino, De Marco, Allazetta, Rinesi, & Bartolini, 1972; Brascamp, van Ee, Pestman, & van den Berg, 2005). Here we go a step further by determining the effects of specific task manipulations in terms of changes in these distributions, thereby covering not only their means but their entire shapes, adding a new dimension that is absent in conventional analyses.

1.1. Dynamics of perceptual bi-stability in relation to the present analysis

A first step to attain an understanding of the dynamics is to identify the perceptual reversal distribution for different

---

* Corresponding author. Fax: +31 30 2522664.
  E-mail address: r.vanee@phys.uu.nl (R. van Ee).
  URL: www.phys.uu.nl/~vanee/ (R. van Ee).

control exertion tasks. To further unmask neural underpinnings it is also important to examine to what extent binocular rivalry and perceptual rivalry produce different data. Such a comparative examination creates an additional constraint on neural models as it is an open question to what extent binocular rivalry and perceptual rivalry share a common mechanism. We have recently collected a data set of about 60,000 perceptual reversals for six subjects across four different control exertion tasks and four types of visual rivalry stimuli (van Ee et al., 2005). Two of them were binocular rivalry stimuli, the other two were perceptual rivalry stimuli (Fig. 1). The control exertion tasks consisted of "natural", "hold", and "speed up" tasks.

Any conclusion on time-varying data may be invalid unless some prerequisites concerning the dynamic properties have been established. First, using Spearman-correlation tests we found that for each of the used tasks and stimuli the acquired reversals were to a considerable extent sequentially independent (van Ee, 2005). Second, the drift of the perceptual reversal rate was limited to a short onset-related period (van Ee et al., 2005). The drift was absent across both successive chunks of reversals and experimental repetitions. Third, eye movements, including microsaccades, and blinks were not related to the perceptual flips for the tested stimuli and conditions (van Dam & van Ee, 2005, 2006), substantiating the assumption that the perceptual reversal process can be central in nature. Finally, we compared various distributions and determined the best fitting distribution to our data, revealing that the reversal rates closely followed a Gamma distribution (Brascamp et al., 2005), providing a tool to further analyze the relationship between the distribution's parameters and

the stimulus or tasks. Here, we analyze the results provided by this tool.

A characteristic of the Gamma distribution is its unimodal, right-skewed profile. It consists of a shape parameter k, and a scale parameter λ (see Appendix A). It was introduced in the field of perception by the seminal work of Levelt (1967) to describe the distribution of perceptual durations. The shape parameter characterizes the skewness of the distribution, while the scale parameter scales the distribution along the abscissa. In our paper we use a Gamma rate (reciprocal duration) distribution because the fit qualities of the rate distributions surpassed those for the duration distributions (Brascamp et al., 2005).

1.2. Aim of this study

We first sought regularities in the Gamma fit parameters across stimuli and voluntary control exertion tasks for the above-described data set. We found that subjects' perceptual reversal rate distributions differed systematically in both parameters, k and λ, for all stimulus and task manipulations. The cardinal component of subject-dependent perceptual reversal rate variation appeared to be not the conventionally used mean rate ($\lambda \cdot k$), but a component that was oriented—for all conditions—roughly perpendicular to the mean rate. Moreover, stimulus variations brought about a diversity of systematic two-parameter effects.

Our characterization of voluntary control effects by the novel two-parameter analysis made us aware of the possibility to examine a hitherto unappreciated indistinctness in voluntary control instructions. More specifically, we did a new experiment in which we employed specific variations in control exertion of either of the two competing percepts for the Necker cube. Again we found that the difference between reversal rate distributions was systematic and reflected the same constraint on the scale and shape parameters as we found for the first experiment. And again, across subjects the perceptual reversal rate distributions varied in the same systematic way, implying that subjects had to a considerable extent independent control over the reversal rate—and all in a similar way—of either of the two competing Necker cube percepts.

2. Experiment 1: Voluntary attentional control for various stimuli and tasks compared

2.1. Methods

Thus, we first analyzed previously reported perceptual reversal responses (van Ee et al., 2005) and fit parameters (Brascamp et al., 2005) using our two-parameter analysis. In short, six subjects participated and four different rivalry stimuli (Fig. 1) were presented to them: Orthogonal grating, House-face, Necker cube, and Slant rivalry (width 1.2° at 114 cm). Subjects were instructed to report reversals and to maintain central fixation. To check whether the sub-
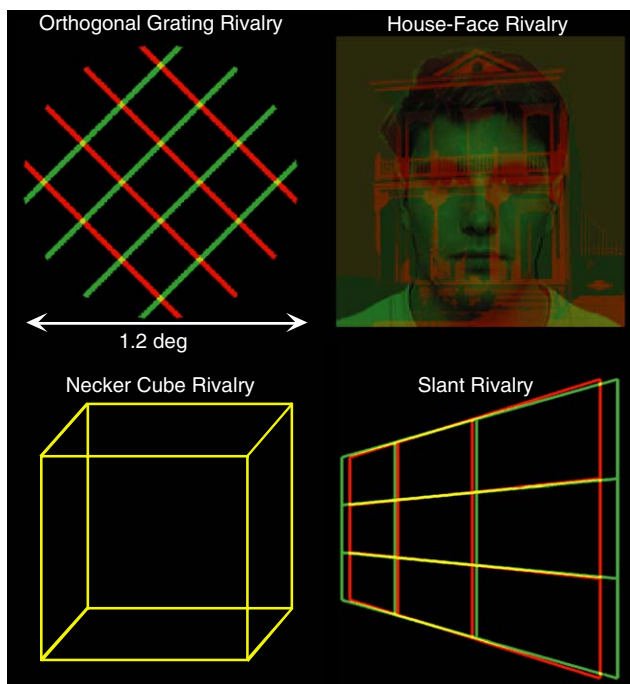

Fig. 1. The four rivalry stimuli studied.

jects were reliably reporting the occurrence of perceptual reversals, so-called 'catch periods' without ambiguity were included. Subjects were given four different tasks: (1) to view a stimulus in a "natural" way without attempting to control the reversal rate, (2) to "hold" one or (3) the other of the two percepts for as great a fraction of the time as possible, and (4) "to speed" up the reversal rate as much as they could.

We analyzed the durations of one percept (e.g., the house) separately from the durations of the other percept (e.g., the face). All these variables taken together, led to 6 (subjects) × 4 (stimuli) × 4 (tasks) × 2 (percepts) = 192 distributions, based upon 59,589 reversals. Each distribution produced two Gamma fit parameters. Those fitted scale and shape parameters are clearly related to one another (Fig. A1 in Appendix A): a cloud of similarly colored symbols, i.e., an experimental condition, is roughly enclosed between the axes (k and λ) and a hyperbola. This implies that only a restricted combination of shape and scale parameters apply.

The main realization underlying our approach is that an entire distribution is defined by one single point in a 2-D space subtended by the shape and scale parameters, providing a concise way of disentangling effects of specific manipulations. The processing steps described in the following sections are intended to further enhance the clarity of this representation.

2.1.1. Logarithmic transformation of Gamma fit parameters

The first stage of our analysis is to determine the logarithm of the fitted shape parameter ($\log k$) versus the logarithm of the scale parameter ($\log \lambda$), transforming any power law relationship ($\lambda \propto k^\alpha$) into a linear relationship ($\log \lambda = \text{const} + \alpha \log k$; see inset in Fig. A1). As a second stage, to bring out both the inter-subject variance structure, and the role of voluntary control, the log-transformed parameter pairs were subjected to a 2-D Principal Component Analysis (PCA) that determined the "natural" coordinates along which subjects differed systematically.

To illustrate these two stages, Fig. 2 portrays two examples, selected to show fit parameter patterns that became either very elongated, with a relatively small influence of the control exertion task (Fig. 2, top for grating rivalry), or that became globular, with distinct effects of the control tasks (Fig. 2, bottom for slant rivalry). Fit parameters for the complete spectrum of possible percepts are shown in Fig. A2. Remarkably, the order of individual subjects within an elongated cloud seems to be pre-
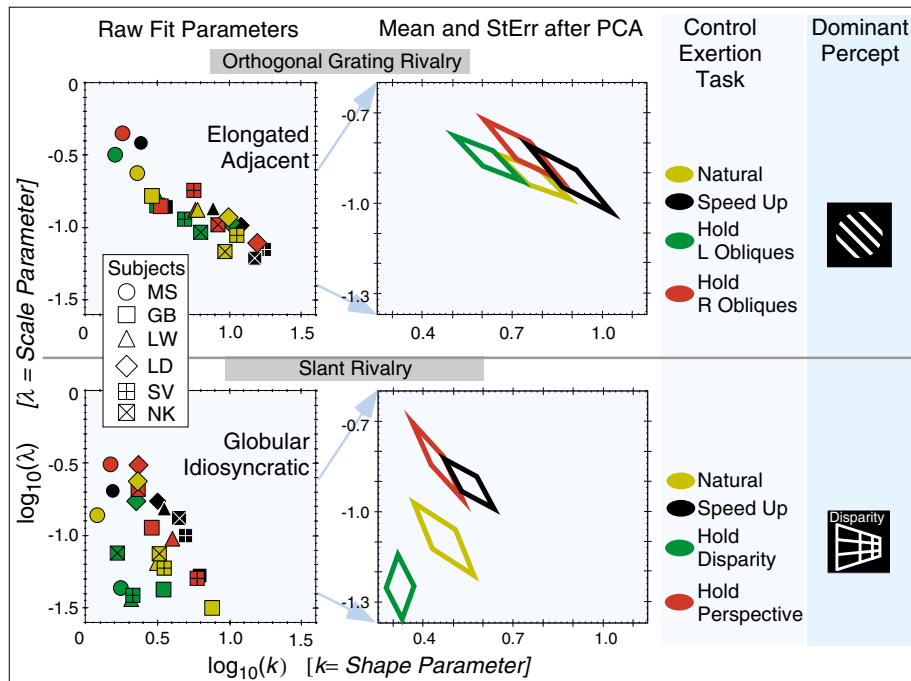

Fig. 2. Two data analysis illustrations: Gamma rate fit parameters in log space and two-dimensional (2-D) Principal Component Analysis (PCA). To arrive at a quantification of the role of voluntary perceptual control in terms of fit parameters we first took the logarithm of the fit parameters (left plots) and then we applied 2-D PCA (right plots). This figure illustrates the merits of our data analysis with two examples from the ends of the spectrum of occurring fit parameter patterns: one that is elongated, with a relatively small influence of the control exertion task (left top), the other is globular, with idiosyncrasy concerning the control tasks (left bottom). The left top graph depicts the fit parameters for grating rivalry when the left grating dominates, the left bottom graph depicts the fit parameters for slant rivalry when disparity dominates. The different colors denote the different control exertion tasks. The different symbols denote the six subjects. Note that the order of individual subjects within an elongated cloud seems to be preserved: generally the disks reside in a cloud in the top-left region and the cross-haired squares reside in the bottom right region. The center of any rhombus in the panels on the right represent the location of the mean across the subjects. The axes, known as PCA axes, of any rhombus denote the major and minor components of the standard errors in the mean across the subjects. Note that the subjects' rank order information gets lost in the PCA analysis.

served: for both grating rivalry and slant rivalry generally the disks reside in a cloud in the top-left region and the cross-haired squares reside in the bottom right region irrespective of the control exertion task. The right panels of Fig. 2 exemplify outcomes of the PCA denoted by the diamond shaped symbols (rhombi), representing the clouds. The center of any rhombus in those panels represents the location of the mean across the subjects. The axes of any rhombus denote the direction and magnitude of the major and minor components of the standard errors in the mean across the subjects. The remarkable preservation of the subjects' ordering within each rhombus implies that the shifts of the rhombi to a large extent characterize also the responses of the individual subjects to the stimulus types and control tasks. Thus, the displacement and scaling of the rhombi provide an efficient characteristic of the effect of task and stimulus on the subjects' distribution fit parameters.

2.1.2. Interpretation of data in log space

Prior to embarking on an analysis of the location, the shape, and the shifts of the rhombi we will first consider the 2-D log space interpretation. Fig. 3 demonstrates how to interpret the shifts in Gamma rate fit parameters for realistic experimental values. The product of the shape and scale parameters ($k \cdot \lambda$) of any Gamma rate distribution is identical to the mean (μ) of the perceptual reversal rate (see Appendix A). Thus, $\log \mu = \log k + \log \lambda$ becomes the main diagonal (red) in Fig. 3. Lines of constant mean rate are perpendicular to this axis. The inset-plots with the gray distribution profiles illustrate how the profile of the rate distributions changed for the spectrum of parameters that occurred in our experiment.

Published analyses of control exertion (including our own) examined changes in the mean perceptual reversal rate. Thus, these analyses collapsed the two-parameter space of the rate distributions onto the mean rate (or μ) axis. However, part of the effects of task and stimulus involves shifts along the axis perpendicular to the μ axis ($\mu^{\perp}$-axis).

Does the direction of data variation along the $\mu^{\perp}$-axis have a genuinely meaningful interpretation? This direction can be expressed as: $\frac{\lambda}{k} = \frac{\lambda^2}{\mu} = \frac{(\mu - m)^2}{\mu}$ (see Appendix A), where m is the *mode* (location of the max) of the distribution. One may note that it has the same dimension $[s^{-1}]$ as the mean rate $\mu = k \cdot \lambda$. Note the structural similarity to the quantity SD^2/μ, that characterizes the variance of the "Gaussian" distribution in relation to the mean. The difference between mode and mean can be considered a measure of asymmetry. The increase along the $\mu^{\perp}$-axis (i.e., towards the top-left) for fixed μ can be interpreted as a decrease in the mode of the distribution. There are three other quantities indicated in Fig. 3 (derived in Appendix A) that help to interpret the shift of the rhombi: changes in the standard deviation or σ, as well as changes in the coefficients of "Skewness" and "Variation" of the distribution, all of which are included as arrows in Fig. 3.
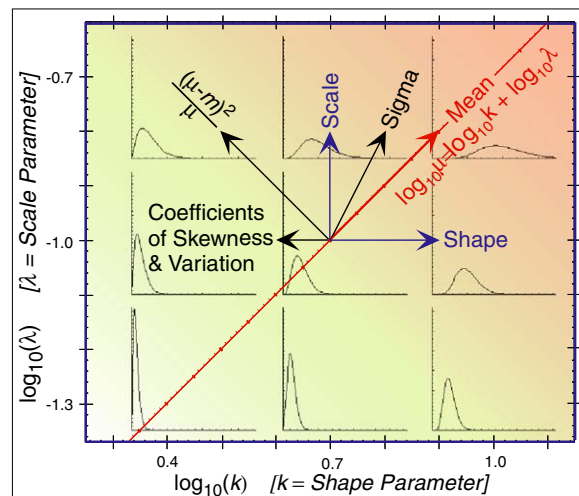

Fig. 3. Fit parameter interpretation in $\log k$ and $\log \lambda$ space. Reversal rate differences between the control exertion tasks were found (Fig. 2) to be conveniently described by a shift in the shape (k) and scale (λ) parameters of the Gamma reversal rate distribution (blue arrows). The product of the shape and scale parameters ($k \cdot \lambda$) is identical to the mean perceptual reversal rate. This mean rate is depicted along the red oblique axis, its scale being $\log_{10} k + \log_{10} \lambda$. The inset-plots demonstrate how the profile of the rate distributions changed in our experiment (compare the scales with the right panels of Fig. 2). From those gray distribution profiles it can be seen that the mean reversal rate increases when going to the right top of the plot. The direction perpendicular to the red axis, where the means stay constant, can be specified in terms of distribution free parameters as $(\mu - m)^2/\mu$, where μ is the mean of the reversal rate distribution, and m (the mode) specifies where the frequency of occurrence is maximal. To further facilitate interpretation of the control exertion-induced shifts, changes in other interesting quantities like sigma, and the coefficients of skewness and variation of the rate distributions are also denoted by vectors, the length of which specifies the relative strength. Note that extant distribution analyses examined changes in the mean, but not in the fit parameters, meaning that those studies have effectively projected their data on the red axis, thereby disregarding one dimension of data changes.

2.2. Results

2.2.1. Mean and standard error of fit parameters across subjects

We applied PCA to the data for all control exertion tasks and for all stimuli separately (see left panels of Fig. 4) to find the mean across the subjects and the major and minor components of the standard error in the mean across the subjects. The different control exertion tasks are denoted by the different colors. The dashed and undashed rhombi (see right column of legend) differentiate the pairs of percepts that competed for dominance. We begin with a description of the pattern of results in the left panels.

A conspicuous finding is that the major PCA axes are roughly aligned with the $\mu^{\perp}$-axis, meaning that the subject variation reflects a constraint on the scale and shape parameters allowing less variation on their product (the mean μ) than their ratio ($\mu^{\perp}$). But more importantly, instructions and stimuli produce a diversity of essentially 2-D shifts in the centers of the rhombi.
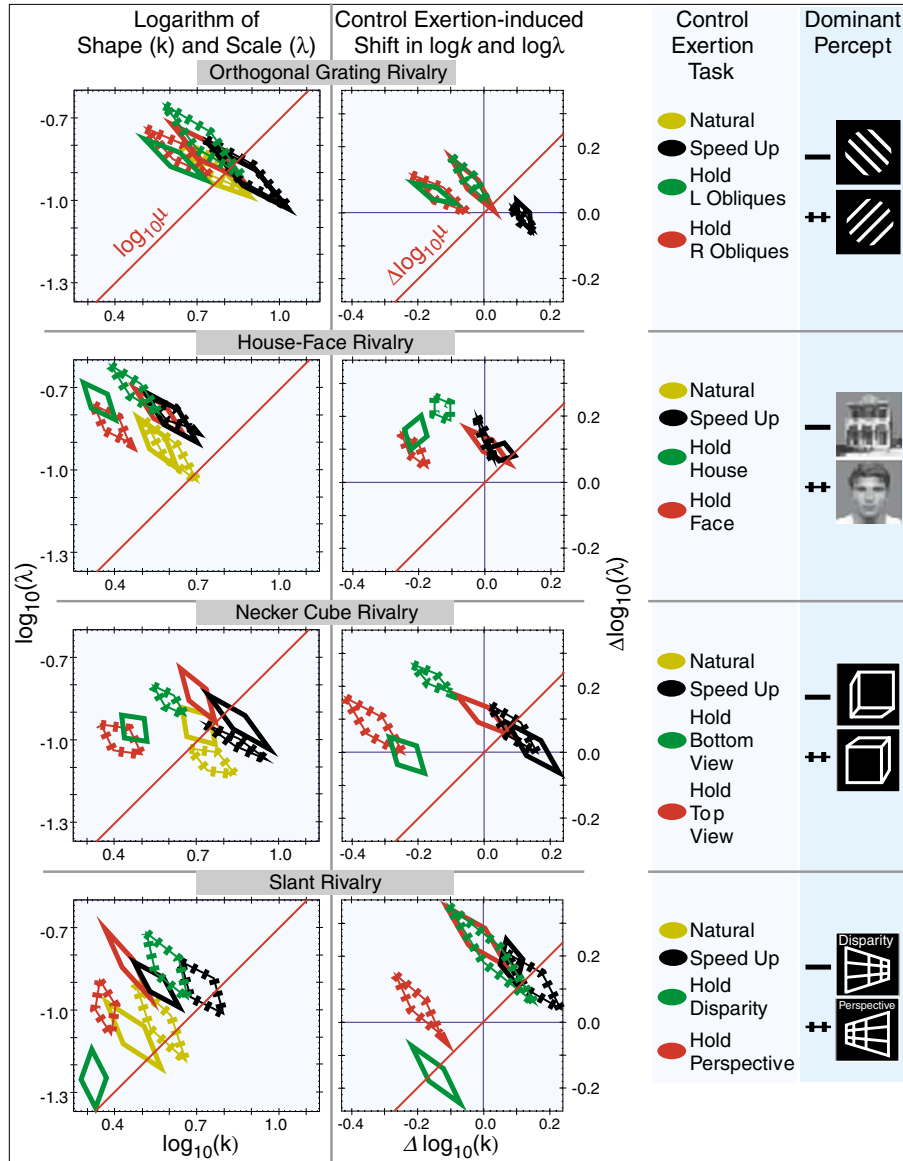
Fig. 4. Mean and standard error of Gamma rate fit parameters after two dimensional Principal Component Analysis (PCA). The rhombi in the four panels on the left represent the fit parameters for the six subjects (note that the representation is the same as in Fig. 2). The rhombi in the four panels on the right represent the six subjects' shifts of the fit parameters for a particular control exertion task relative to the natural control exertion task (the latter being at the origin). As in Fig. 2, the center of any rhombus denotes the location of the mean across the subjects. The axes, known as PCA axes, of any rhombus denote the standard errors in the mean across the subjects as derived from the 2-D probability density distribution used in PCA. The different colors denote the different control exertion conditions. From top to bottom the four sets of graphs depict the fit parameters for grating, house-face, Necker cube, and slant rivalry. The dominance of the two alternative percepts is denoted by dashed and undashed rhombi (see right column of legend). The red oblique axes denote the direction along which the mean, μ, of the fitted distribution changes. When going from grating rivalry to slant rivalry there is an increase in both the variability of the means (the colored rhombi become more distinct) and the inter subject variability (the rhombi become larger), meaning that the role of voluntary control becomes increasingly greater and the subjects perform increasingly different, respectively. The major PCA axes appear to be aligned perpendicular to the—traditionally used—mean axis, meaning that the subject variation reflects a constraint on the scale and shape parameters allowing less variation on their product than their ratio.

Concerning the "natural" and the "speed up" control exertion tasks (yellow and black rhombi), one may expect—based upon stimulus and percept symmetry considerations—that the distributions for the two competing percepts (dashed and undashed) will be roughly similar. Indeed for binocular rivalry (grating, house-face) the dashed and undashed rhombi are superimposed in black and yellow. There are, however, interesting exceptions for

the other stimuli. For the Necker cube, the "speed up" task is slightly more successful for the bottom view, as the dashed black rhombus is placed somewhat lower along the μ axis. More interestingly, the rhombi for the "natural" percepts are shifted along the vertical direction, meaning that the shape parameter is nearly identical and the scale parameter is different. For Slant Rivalry, the rhombi for the competing percepts are not superimposed at all for

the "natural" and "speed up" tasks, meaning that there is a clear bias for the disparity-dominated slant percept in both tasks.

Concerning the "hold" control exertion tasks (red and green rhombi), one would expect that the rhombi for the two competing percepts are shifted relative to one another along the μ axis. Indeed, the dashed and undashed rhombi (of one color) do not superimpose for these tasks. There is clearly a progression in the extent of the shift between the dashed–undashed pairs of rhombi of the same color when one moves from the upper towards the lower panels, meaning that subjects are more effective in holding a percept for Slant and Necker cube rivalry than for the grating and house-face rivalry. An important feature is that (with exception of the hold disparity-slant task) the rhombi for the hold tasks are displaced relative to one another parallel to a μ axis (that is up and leftward relative to the μ axis through the "natural" rhombi). This means that a major effect of the hold task is an increase of the asymmetry of the distribution for either percept (note that the displacement can be interpreted as an increase in $\mu - m$).

Collectively, when going from grating rivalry to slant rivalry there is an increase in the effect of voluntary control exertion tasks on the reversal rate distributions, as witnessed by the rhombi becoming more distinct. In addition, the inter-subject variability increases, as witnessed by the rhombi becoming larger. These findings, in turn, mean that the effect of voluntary control instructions becomes increasingly more idiosyncratic and that the subjects perform increasingly different, respectively. To validate our data processing method we performed Monte Carlo analyses. We found that the PCA components found for Monte Carlo generated data distributions were a factor of 10 smaller than the results for the real data across the complete space of our experimental data. In other words, fitting errors or noise are not responsible for the patterns we report.

2.2.2. The role of voluntary control quantified

We took one final step in data processing to bring out the effect of instructions. For each individual we calculated such effects in terms of the difference in $\log k$, and the difference in $\log \lambda$ relative to the "natural" task (which is located at the origin). Then we applied again a PCA analysis to these differences. The panels on the right in Fig. 4 depict how a task shifts the population of rate distributions relative to the "natural" task distributions for the same percept and stimulus condition. We first point out that generally the length of the long PCA axes are remarkably small, implying that the order of subjects within the rhombi for the "natural" task (yellow rhombi in the left column) is very similar to the order within the rhombi for the other tasks (the axes would have been about 10 times longer from the PCA analysis if subjects were ordered independently across rhombi).

The task always caused a shift in $\log k$ and/or $\log \lambda$ (none of the rhombi is located at the origin). The "speed up" task (black rhombi) caused shifts in various directions relative

to the 'natural' task. These directions were roughly the same for the competing percepts (dashed and undashed) but depended on the stimulus: an increase of shape (Grating, Necker cube), an increase of scale (House-face), or an increase of both (Slant rivalry).

The hold task, if successful, ought to shift the held percept (green undashed and red dashed rhombi) differently than the alternative 'left free' percept (green dashed and red undashed). This was indeed the case for all conditions. For the grating stimulus the shift was identical for the pair of held (or left free) percepts, as evident from the overlap of these rhombi (e.g., Fig. 4, upper right panel; rhombi for held percepts, and for left free percepts overlap). The shift also depended on which percept was held (left free). An interesting example is found for the slant rivalry condition. Hold-perspective evoked a pure left-shift in *shape* for the perspective percept (red dashed); in contrast hold-disparity evoked a pure shift of the *mean* for the disparity percept (green undashed). For either task a pure upward shift in scale occurred for the percept that was left free (Fig. 4, lower right panel). Note that although the hold task refers to just one percept that the distributions for the other percept were also shifted: none of the percepts that were left free (dashed green and undashed red rhombi) were located at $(0,0)$. Finally, a striking observation (for perceptual rivalry) is the alignment along the $\mu^\perp$ direction of the "speed up" rhombi and the rhombi for the percepts that were not held. Apparently the non-held percepts for these tasks increased in rate by nearly as much as the percepts for the "speed up" task even though there is a clear distinction in the distribution's profile. In Experiment 2 we will examine this in detail by specific but subtle variation of the hold task.

Collectively, it appears that the two reversing percepts (the dashed and undashed rhombi) seem to be more overlapping for the binocular rivalry stimuli than for the perceptual rivalry stimuli, irrespective of the task and even for the physically symmetrical Necker cube stimulus. Further, to hold a percept (the red and green rhombi) all subjects effectively altered both the shape and the scale parameters, and they all did this with similar amplitude for each particular percept. There is more inter-subject variability in doing so for perceptual rivalry than for binocular rivalry given that the rhombi for perceptual rivalry are generally larger than those for binocular rivalry.

2.2.3. Subjects' rank order preservation

We have seen so far clear indications of preserved rank order of individual subjects across experimental conditions. In other words, a subject who is a fast switcher relative to other subjects for one condition is also a relatively fast switcher for another condition. Here, we used Spearman rank correlation to systematically examine the preservation of subject rank order across conditions.

To systematically examine rank order preservation we first ranked a subject's pair of fit parameters (shape, scale) among the other five subjects' pairs, for each separate con-

dition (see Appendix A for details). The long and the short PCA axes of the rhombi serve as the natural projection axes for such ranking. We then determined the correlation coefficients between pairs of six rank numbers. The rank correlation coefficients for the compared conditions are presented in Fig. 5. To assess whether a histogram associated with a particular tested factor specifies that there is preserved rank order, we determined the corresponding histogram (with the same bin size) for the so-called "exact

Fig. 5. Subjects' rank order preservation across conditions. The histograms portray the number of occurrences of a Spearman rank correlation coefficient as calculated from pairs of conditions. (A) portrays the exact null-distribution that we use for reference to assess the (lack of) random rank correlation of the other histograms: the null-hypothesis specifies that there is no preserved rank ordering, entailing a histogram that constitutes the 720 (6 factorial) possibilities for which one can randomly rank two sets of 6 subjects. Note that the null-distribution's variations are due to fine structure akin to the correlation process; any other histogram contains similar variations, but also sampling noise. To rank a subject's fit parameters among the other five subjects' parameters we used one of three possible projection axes: the long (left column) and the short (middle column) PCA axes of the previously produced rhombi, as well as the mean rate axis (right column). (B) The first row portrays the number of occurrences of a rank order correlation coefficient for correlation across control exertion tasks, with the 'natural' task as reference. The second row portrays the number of occurrences across the different stimuli (light gray), with the grating stimulus and the 'natural' task as reference. Of the 24 coefficients per plot of the second row, eight coefficients are being associated with the correlation of grating and house-face stimuli (black, with the relatively high correlation coefficients), which both belong to the class of binocular rivalry stimuli. The third row portrays the correlation coefficients across complementary percepts. The generally positive correlation coefficients demonstrate that the rank order of subjects is for a considerable part preserved across control exertion tasks, stimuli, and complementary percepts.

null-distribution" specifying that there is no such preservation. The number of different ways in which one can randomly rank 6 subjects across two sets amounts to 720 (6 factorial) entailing a histogram that is depicted in Fig. 5A.

Fig. 5B displays the histograms of the rank correlation coefficients. The results for projection on the long PCA axis are in the left column, and those for the short PCA axis are in the middle column. In addition, we have calculated the rank correlations after projection on the mean rate axis (right column) for comparison with the traditional analyses that focused on differences in the mean reversal rates. The first row quantifies the rank order correlation across control exertion tasks, demonstrating that the correlation coefficients are all, but one, positive. The second row shows that, across the different stimuli, there is generally a positive correlation. The black bars show that the preservation of rank order across the grating and house-face stimuli is slightly greater than the preservation across the grating and the perceptual rivalry stimuli. Note also that across stimuli there are few negative correlation coefficients. The coefficients in the third row show that those are not being caused by the complementary percepts because here other negative coefficients show up.

Collectively, the obvious difference with the exact null-distribution, in conjunction with the generally positive correlation coefficients, allow us to conclude that the rank order of subjects for each of the three projective axes was for a considerable part preserved across control exertion tasks, stimuli, and percepts.

3. Experiment 2: Do subtle variations of "hold" instructions reveal specific control?

3.1. Methods

In the previous experiment, we found that the given instruction "hold this percept for as large a fraction of time as possible" encouraged subjects to modify not only the parameters of the rate distribution for the held percept but also those for the complementary percept. An interesting question is whether the subjects sped-up the non-held percept because there exists a genuine limitation on the control of distributions of a single percept, or simply because subjects believed that holding one and speeding up the other was the preferred interpretation of our (ambiguous) hold-instruction. We asked seven subjects, all different from the ones used in the previous Experiment, to perform the hold task in specific ways. The control exertion tasks, which are tabulated in the inset of Fig. 6, were fourfold: (1) natural viewing for both bottom and top view percepts (yellow, just as before); (2) hold bottom view, and no specific control for the top view, which ought to be similar to the instruction in Experiment 1 (green, just as before); (3) hold bottom view, and natural control for the top view (pink); (4) natural control for the bottom view, and speed up for the top view (brown).
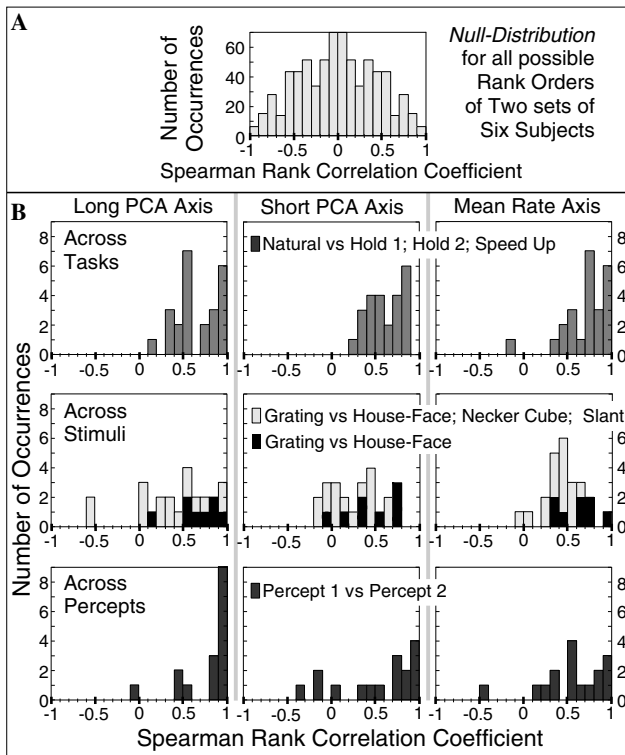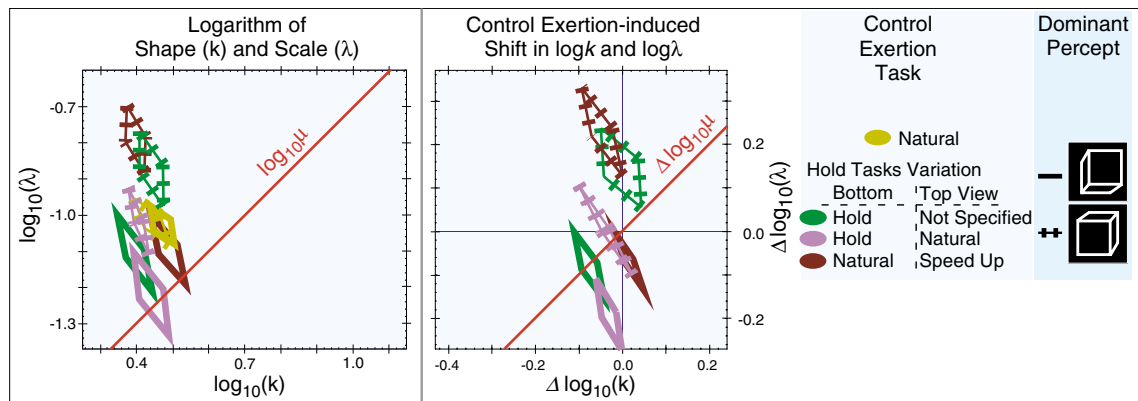
Fig. 6. Experiment 2: Mean and standard error of Gamma fit parameters after 2-D Principal Component Analysis. As Fig. 4 but for Experiment 2 in which we varied the "hold" control exertion task. The rhombi in the panel on the left represent the fit parameters for the seven subjects. The rhombi in the panel on the right represent the subjects' shifts of the fit parameters for a particular control exertion task relative to the natural control exertion task. The different colors denote the different control exertion conditions. The dominance of the two alternative percepts is denoted by dashed and undashed rhombi. Variation of the 'hold' task appears to involve mainly the scale parameter.

We focused on the Necker cube because for this stimulus we obtained clear voluntary control effects in Experiment 1 (Fig. 4). The cube's size (8.2° at a distance 62 cm) was deliberately larger than in Experiment 1: first because the reversal rate decreases with the cube's size (Borsellino et al., 1982), thereby providing potentially better conditions to tease apart the effects of voluntary control; second to validate our methods it is worth to examine whether a stimulus that differs only in size, but that is further similar produce data patterns similar to those found in Experiment 1. A total of at least 300 perceptual reversals were collected for each condition for each subject.

Existing analyses of the fixation positions at about the moment of the perceptual flips indicate that the fixation position by itself does not determine the percept but that subjects prefer to fixate at different positions when asked to hold either of the different percepts (Toppino, 2003; van Dam & van Ee, 2006). It is crucial to examine whether the separate control is not just reflecting different eye movement strategies. Gaze data for three subjects were collected using an SMI Eyelink data acquisition system at 250 Hz while subjects performed the task.

3.2. Results

Fig. 6 portrays the results for the seven subjects in terms of $\log k$ (shape) and $\log \lambda$ (scale) in a format that is identical to the previously used format for Fig. 4 (see Fig. A3 for raw data in terms of k and λ). The reversal rates in Experiment 2 for the larger cube were indeed clearly slower than those found in Experiment 1 (this becomes particularly clear once the projection on the red $\log \mu$ axis in the left panel of Fig. 6 is considered), although the different sets of subjects might also play a role. Nevertheless, comparison of the green rhombi for the Necker cube in the right panel of Fig. 4 with the green rhombi in the right panel of Fig. 6 demonstrates that the data are similar: the location of the dashed green rhombus is different from the loca-

tion of the undashed rhombus mainly in terms of the scale parameter. Moreover, although both the dashed and undashed green rhombi in Fig. 6 are displaced relative to the dashed and undashed green rhombi in Fig. 4, in terms of both the location and the shape of the rhombi, the data are about identical in both plots (the shift in $\log \mu$ amounts to 0.3 in both plots; in terms of the shift in shape and scale parameters this shift is also identical in both plots).

Subjects were quite able to control each percept separately. As shown in the right panel of Fig. 6, the rhombi for the instruction 'natural' (pink-dashed and brown-undashed) remained very close to (0,0), while the rhombi for the competing percept that was held (pink-undashed) or sped-up (brown-dashed) shifted away from the origin in the instructed direction. Subjects were again well able to execute the previously (Experiment 1) used "hold" instruction (green rhombi). The most conspicuous finding is that across tasks the rhombi are mainly shifted in their λ parameter values relative to one another, meaning that mainly the time-scale parameter, but not the family-shape parameter is being modified while exerting the "hold" control.

The gaze recordings of all three subjects demonstrated that there were no systematic differences in fixation location during either of the two percepts across the voluntary control conditions: in all cases the p value (2-sided t test) exceeded .01, and for just one subject and only one condition the p value fell below .05. In addition, the moment of a perceptual alternation was clearly not causally related to blinks. We cannot rule out, however, that small saccades may have contributed to trigger a perceptual alternation. Yet, given the similarity of the average fixation location in our conditions and existing consensus for Necker cube eye movements analyses (Toppino, 2003; van Dam & van Ee, 2006), it seems appropriate to conclude that the control over perception was predominantly the result of central mechanisms. Note, regardless the role of eye movements, our two-parameter analysis is indispensable to disentangle effects for the various conditions.

We conclude that our observation that the 'hold' instruction in the first experiment evoked slower rates for the held percept but higher rates for the other percept was not caused by an intrinsic limitation to control the competing percepts only pair-wise. Rather, observers do seem to have to a considerable extent independent control over the reversals of either percept, at least for the Necker cube.

4. Discussion

To study the dynamics of perceptual reversals, as well as the role of voluntary control, we have exploited the full 2-D characterization offered by the Gamma reversal rate distribution's parameters (shape and scale) across differences in both stimuli and voluntary control exertion. This approach offers a concise way of addressing effects of specific manipulations on the entire reversal rate distribution, rather than merely its mean. We found both for existing and new experimental data that the subject-dependent component of data variation reflects a constraint on the scale and shape parameters allowing less variation on the product than on the ratio of the scale and shape parameters. Moreover, instructions and stimuli produced a distinct diversity of essentially 2-D shifts in scale and shape parameters. Our 2-D analysis of perceptual bi-stability, and its voluntary control, reveals a variety of systematic effects that would have been invisible to conventional analyses but that critically constrain models of bi-stable perception. For the Necker cube (Experiment 2) our 2-D analysis revealed that all our seven subjects had to a considerable extent independent voluntary control over either of the two competing percepts.

4.1. Conventional and new analyses compared

The subject-dependent component of data variation is roughly perpendicular to the traditionally used mean rate. There is no straightforward existing statistical measure that relates to this direction of data variation. We have derived an equation (Appendix A) that relates this direction of data variation to the difference between the mode (location of the top) and the mean of a perceptual reversal rate distribution. The magnitude of this variation can thus be associated with what a subject does on average (the mean) related to what a subject does most often (the mode).

Previous psychophysics analyses, including our own, have focused their attention on data variations along the increasing mean reversal rate axis.[1] Thus, extant analyses have effectively projected the data on the mean axis (the

---

[1] There are two exceptions: an early and a very recent analysis by Borsellino et al. (1972) and Mamassian and Goutcher (2005), respectively. The former did not seek regularities across different conditions, although it went as far as correlating the shape and scale parameters to one another; the latter concentrated on percept survival analyses. Both studies suggest though that the reversal distributions can be described by one parameter.

red axis in Fig. 3). Indeed the current results replicate the found mean perceptual reversal rates from our previous data analyses within one standard error (Table 2 in van Ee et al., 2005). Most of the found effects in the current paper would not have shown up with conventional analyses. For example for the Necker cube data (third panel on the right of Fig. 4) the traditional projection would imply that there are no differences between the competing percepts (dashed and the undashed rhombi).

Another feature that conventional analyses might not detect is the variation in the perceptual reversal rate distribution when the hold control exertion is varied in a subtle way (Experiment 2, where we asked subjects to influence the dominance period of one of the two competing Necker cube percepts independently from the other percept). We found under such variation that mainly the scale parameter varied in a way that was clearly distinct across the variations in control exertion, whereas the conventional mean rates were less distinct (Fig. 6). Note that the result of a change in the scale parameter (with constant shape parameter) for a rate distribution's profile is identical to a change in the scaling of the reciprocal time axis.

4.2. Various perceptual rivalry paradigms compared

In recent literature on bi-stable perception, much attention has been directed towards answering the question whether binocular rivalry on the one hand, and perceptual rivalry on the other, reflect either distinct or similar neural mechanisms. An oft-repeated argument in this discussion in favor of similar neural mechanisms is that percept durations have similarly shaped distributions in both binocular rivalry and perceptual rivalry. Our 2-D way of examining data adds details to this discussion. Collectively, for our data it appears that the two reversing percepts (represented by the dashed and undashed rhombi in Fig. 4) are slightly more similar for the binocular rivalry stimuli than for the perceptual rivalry stimuli, irrespective of the task. For example, although both the Grating and the Necker cube consist of symmetrical competing interpretations, the shift for the Necker cube is larger. Further, to hold a percept (see the red and green rhombi in Fig. 4) all subjects effectively altered both the shape and the scale parameters and there is slightly more inter-subject variability in doing so for perceptual rivalry than for binocular rivalry.

We have compared the rank order preservation of subjects across experimental conditions. The rank order of our six subjects for both binocular rivalry and perceptual rivalry was for a considerable part preserved across control exertion tasks, stimuli, and percepts, which is consistent with another recent study (Carter & Pettigrew, 2003), that focused on the subject order preservation across stimuli. It is noteworthy though that we found clear correlation using, statistically speaking, only a few subjects because Carter and Pettigrew tested as much as 61 subjects and found a correlation coefficient of 0.69, leaving little hope to find positive correlation across our few subjects. Fig. 5 shows

that we found highly significant preservation of rank order across stimuli, which was slightly higher across the grating and house-face stimuli than it was for the preservation across the grating and the perceptual rivalry stimuli.

The found patterns demonstrate that there are common attentional control effects for binocular rivalry and perceptual rivalry, consistent with the idea that binocular rivalry and perceptual rivalry share at least at some level a common mechanism (cf. Andrews & Purves, 1997; Carter & Pettigrew, 2003; Helmholtz, 1866; Logothetis, Leopold, & Sheinberg, 1996; McDougall, 1906; Walker, 1978). But there appears to be also a role of specific binocular rivalry based mechanisms in that it seems to be harder to control binocular rivalry than figural rivalry (cf. Blake, 1988; George, 1936; Meng & Tong, 2004; van Ee et al., 2005; Washburn & Gillette, 1933). One extensive study on the role of meaning in binocular rivalry even reported that focused attention on linguistically meaningful features did not at all prolong percept dominance (Blake, 1988). It is relevant to note that another study did report significant average effects up to 65% for the "speed up" task in horizontal-vertical bar binocular rivalry when observers were asked to concentrate on either of the two bars (Meredith & Meredith, 1962).[2] But there is the possibility that this study may be flawed as specific eye movements may have occurred. Indeed we have recently demonstrated that for binocular rivalry, more than for figural rivalry, there is a marked positive temporal correlation between saccades and perceptual alternation at about the moment of an alternation (van Dam & van Ee, 2006). This finding constitutes a challenge for some of the existing binocular rivalry voluntary control studies (beginning with the line counting task of Helmholtz (1866)) that have been performed without precise eye posture measurements. Here we demonstrated that, although binocular rivalry stimuli produced significant effects, there were smaller inter-subject effects as well as smaller shifts in scale and shape parameters than for figural rivalry. Further, cognitively meaningful ambiguous figures seem to be better controllable than abstract figures (Strüber & Stadler, 1999) and (local) stimulus configuration can bias perceptual reversal rate (Peterson & Hochberg, 1983; Suzuki & Peterson, 2000; Suzuki & Grabowecky, 2002).

Finally, in forthcoming work we examined the scale and shape parameters of the perceptual reversals instigated by the ambiguously rotating sphere (that can be perceived to rotate either clock wise or counter clock wise, depending on attentional influence (Hol et al., 2003)). Those distribution parameters demonstrated the same relation—or constraint—as described in the present paper, generalizing our present findings. It is noteworthy that the two-parameter analysis facilitated an interesting conclusion that voluntary perceptual control depends on the physical parameters constituting the stimulus (Brouwer & van Ee, 2006), a finding that places important constraints on the mechanisms mediating voluntary control as these mechanisms cannot operate independently of stimulus characteristics. The two-parameter analysis also demonstrated that the greatest variation in data occurred perpendicular to the conventionally used mean rate axis, and in a subject-specific manner. Thus, for the sphere, too, the magnitude of the parameter variation can be associated with what a subject did on average (the mean) related to what a subject did most often (the mode).

5. Conclusion

We have exploited the full 2-D characterization offered by the fitted Gamma reversal rate distribution's shape and scale parameters across the different bi-stable stimuli and different voluntary control exertion tasks. We found that subjects' perceptual reversal rate distributions differed from one another for a particular stimulus and control exertion task in a systematic way that reflects a constraint on the scale and shape parameters. A cardinal subject-dependent component of data variation is not the traditionally used mean rate, but a component roughly perpendicular to it. This component reflects a constraint on the scale and shape parameters allowing less variation on the product than the ratio of the scale and shape parameters. We have derived an equation which relates this direction of data variation to the difference between the mode (location of the maximum) and the mean of a perceptual reversal rate distribution. The magnitude of this variation could in this way be related to what a subject does on average (the mean) and what a subject does most often (the mode).

In addition, stimulus variations induced an interesting diversity of systematic two-parameter effects but the important finding is that all subjects appear to alter the perceptual reversal rate distribution in the same systematic way. In addition, for the Necker cube (Experiment 2) our analysis revealed that all our seven subjects had to a considerable extent independent voluntary control over either of the two competing percepts. Those systematic effects would have remained invisible to conventional mean reversal rate analyses but are critical in constraining models of bi-stable perception. Thus, parametrical analyses across different tasks and different stimuli are informative for studies of awareness as a normal quantifiable biological phenomenon.

---

[2] After we finished this manuscript relevant psychophysics has been reported on increased endogenous control for binocular rivalry when observers pay attention to stimulus features (Chong, Tadin, & Blake, 2005; Chong & Blake, in press).

Appendix A.

A.1. Theory

The probability density function of the Gamma reversal rate (r) distribution is given by $f(r|k,\lambda) = \frac{1}{\lambda^k \Gamma(k)} r^{k-1} e^{(-\frac{r}{\lambda})}$ (where $\Gamma(n) = (n-1)!$ for positive integers, and $\Gamma(n) = \int_0^\infty t^{n-1} e^{-t} dt$ for non-integers). Its two parameters, k and λ, are the shape and the scale parameter, respectively. The shape parameter characterizes the skewness of the distribution, while the scale parameter scales the distribution along the abscissa. Our analyses capitalize on the two-dimensional (2-D) relationship between these parameters. The following expressions are helpful for such analyses. The mean, μ, is related to the distribution parameters as $\mu = k \cdot \lambda$; or, $\log \mu = \log k + \log \lambda$, corresponding to a vector $(1,1)$ in $\log k$, $\log \lambda$ space. The standard deviation yields $\sigma = \lambda \sqrt{k}$; in log space this is $\log \sigma = (1/2)\log k + \log \lambda$, corresponding to a vector $(0.5, 1)$. The "Coefficient of Skewness" is defined as μ_3/σ^3, where μ_3 is the third central moment of the distribution. This yields $\mu_3/\sigma^3 = 2/\sqrt{k}$; in log space this is $-(1/2)\log k$, corresponding to a vector $(-0.5, 0)$. The "Coefficient of Variation" is defined as $\sigma/\mu = 1/\sqrt{k}$; in log space this is again $-(1/2)\log k$, corresponding also to a vector $(-0.5, 0)$. The mode, m, is the location of the maximum: $m \equiv r_{\max} = \lambda(k-1) = \mu - \lambda$.

Most importantly, the direction perpendicular to the mean rate axis can therefore be expressed as: $\frac{\lambda}{k} = \frac{\lambda^2}{\mu} = \frac{(\mu-m)^2}{\mu}$.

A.2. Gamma fit parameters

To determine the best fitting shape and scale parameters of the Gamma rate distribution we employed the least squares method, minimizing the sum of squared residuals. For fitting we used the cumulative probability distribution (CDF) because, as opposed to the probability density distribution (PDF), the CDF does not depend on arbitrary bin size. For the fits we obtained in this manner, we calculated the fit quality pKS, using the Kolmogorov–Smirnov test, which involves the largest overall deviation between the found data and the fitted distribution (for details on this method see Brascamp et al., 2005 & van den Berg & van Loon, 2005).

Fig. A1 portrays how the best fitted scale (λ) and the shape (k) parameters relate to one another. The different rivalry stimuli are denoted by different symbols (see grey top inset of the legend). The different control exertion tasks are denoted by different colors (see blue inset of the legend). For each particular condition there are six identical symbols corresponding to the six subjects. The top graph depicts the fit parameters for one of the two bistable percepts for the grating, the house-face, the Necker cube, and the slant rivalry stimuli. The bottom graph depicts the fit parameters for the alternative of the two bistable percepts. It is not straightforward to interpret these data but on first glance the two parameters seem to be related to one another roughly through a hyperbol-

Fig. A1. The Gamma rate fit parameters of Experiment 1.

ically shaped cloud, implying that only a restricted set of shape and scale parameters describe the perceptual reversal phenomenon. Note that if the data of the six subjects for one particular condition would lie on a perfect hyperbola the two-parameter Gamma rate fit would effectively be promoted to a one-parameter fit. Although it appears to be the case that the triangles (slant rivalry) reside in the plot more to the bottom left part than the squares (grating rivalry) do, generally the clouds overlap and based upon these data it is hard to state that the different conditions produce different data. Note, however, that a power law relationship transforms into a linear relationship if the logarithm of the scale and shape parameters are pitted against one another (see inset in the lower plot). Not only
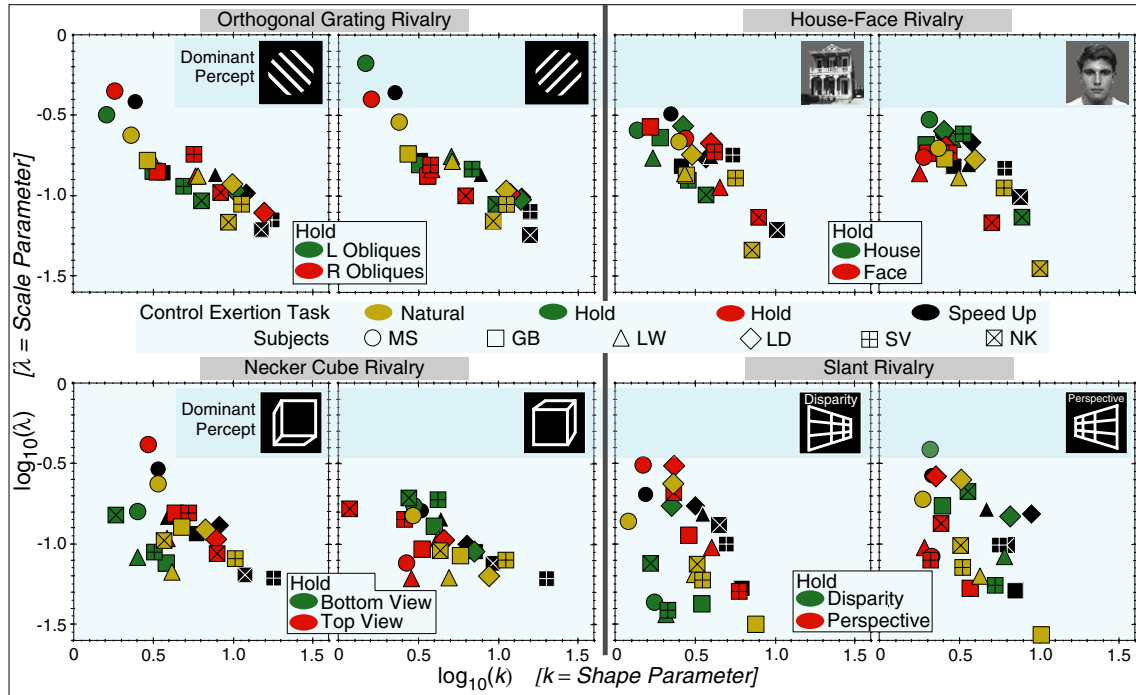
Fig. A2. Gamma rate fit parameters of Experiment 1 in $\log(k)$ and $\log(\lambda)$ space.

do relationships become linear through this transformation but details for small shape and scale parameters become more pronounced.

Fig. A2 portrays the Gamma rate fit parameters in $\log(k)$ and $\log(\lambda)$ space. The left top graphs depict the fit parameters for grating rivalry, separated by the dominant percept. The other top graphs portray the parameters for house-face rivalry; the bottom graphs portray the parameters for Necker cube rivalry and slant rivalry. The different colors denote the different control exertion tasks. The results for the six subjects are explicitly presented by the different symbols. The logarithm of the scale parameter pitted against the logarithm of the shape parameter reveals more structure than we saw when the raw shape and scale parameters were plotted (Fig. A1). For grating rivalry (left top panels) the data seem to confine to a linear relationship and the role of control seems to be hardly significant. The clouds become less structured and the role of control becomes more pronounced when going from grating rivalry to house-face rivalry on to Necker cube rivalry and then to slant rivalry. For slant rivalry the colored clouds consisting of the six subjects' parameters seem to be more distinct. Note that the order of individual subjects within an elongated cloud seems to be preserved: generally the disks reside in the cloud in the top-left region and the cross-haired squares reside in the bottom right region.

Fig. A3 portrays the raw Gamma rate fit parameters of Experiment 2, in which we varied the hold control exertion task. For each particular condition there are seven identical symbols corresponding to the seven subjects.
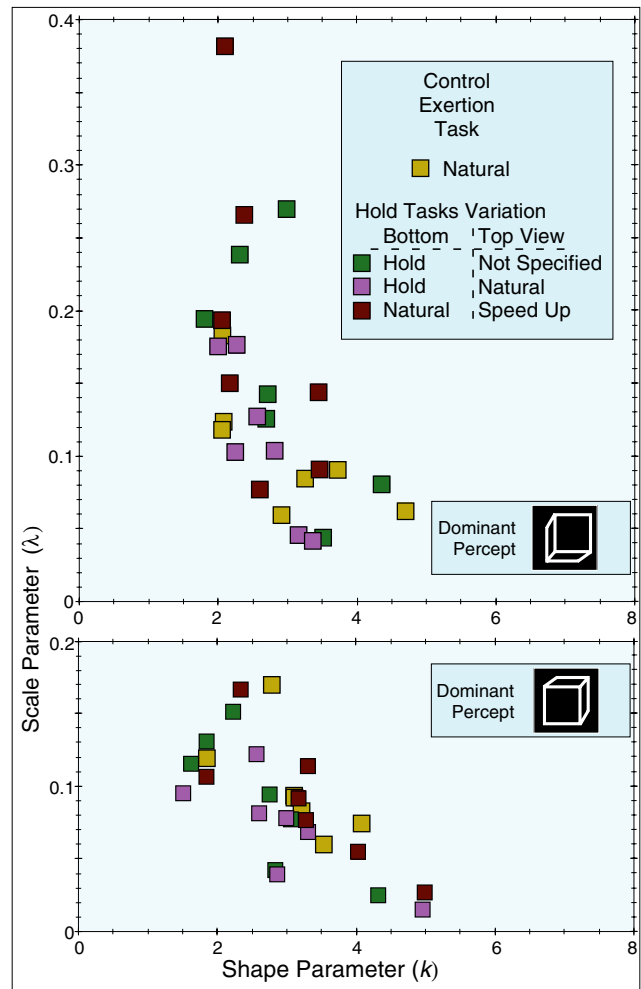

Fig. A3. The Gamma rate fit parameters of Experiment 2.

A.3. Rank correlation

Spearman rank correlation was used to systematically examine the preservation of subject rank order across conditions. To determine the order preservation across the four control exertion tasks we correlated for a fixed combination of stimulus and percept the rank order across the four different tasks with the "natural" task as reference. This gives rise to 4 (stimuli) × 2 (percepts) × 3 other tasks, amounting to 24 correlation coefficients (just as there are 24 "non-natural" experimental conditions—i.e., non-yellow—rhombi in the four left panels of Fig. 4). Next we determined the rank order correlation coefficients across the different stimuli. For a fixed task and percept we correlated across the four different stimuli with the grating stimulus as a reference, again giving rise to 4 (tasks) × 2 (percepts) × 3 other stimuli, amounting to 24 correlation coefficients. Finally, the correlation across complementary percepts (for a fixed task and stimulus) involved 4 (tasks) × 4 (stimuli) with the undashed rhombi as reference, amounting to 16 coefficients (just as there are 16 dashed rhombi in the four left panels of Fig. 4).

References

Andrews, T. J., & Purves, D. (1997). Similarities in normal and binocularly rivalrous viewing. *Proceedings of the National Academy of Sciences of the United States of America, 94,* 9905–9908.

Blake, R. (1988). Dichoptic reading: the role of meaning in binocular rivalry. *Perception & Psychophysics, 44,* 133–141.

Borsellino, A., De Marco, A., Allazetta, A., Rinesi, A., & Bartolini, B. (1972). Reversal time distribution in the perception of visual ambiguous stimuli. *Kybernetik, 10,* 139–144.

Borsellino, A., Carlini, F., Riani, M., Tuccio, M. T., De Marco, A., Panengo, P., & Trabucco, A. (1982). Effects of visual angle on perspective reversal for ambiguous patterns. *Perception, 11,* 263–273.

Brascamp, J. W., van Ee, R., Pestman, W. R., & van den Berg, A. V. (2005). Distributions of alternation rates in various forms of bistable perception. *Journal of Vision, 5,* 287–298.

Brouwer, G.J., & van Ee, R. (2006). Endogenous influences on perceptual bistability depend on exogenous stimulus characteristics. *Vision Research.* in press, doi:10.1016/j.visres.2006.03.016.

Carter, O. L., & Pettigrew, J. D. (2003). A common oscillator for perceptual rivalries? *Perception, 32,* 295–305.

Chong, S. C., Tadin, D., & Blake, R. (2005). Endogenous attention prolongs dominance durations in binocular rivalry. *Journal of Vision, 5,* 1004–1012.

Chong, S.C., & Blake, R. (in press). Exogenous attention and endogenous attention influence initial dominance in binocular rivalry. Vision Research.

George, W. (1936). The significance of the fluctuations experienced in observing ambiguous figures and in binocular rivalry. *Journal of General Psychology, 15,* 39–61.

Helmholtz, H. 1866. *Handbuch der Physiologischen Optik,* Vol III, Sec 32. Hamburg: Voss.

Hol, K., Koene, A., & van Ee, R. (2003). Attention-biased multi-stable surface perception in three-dimensional structure-from-motion. *Journal of Vision, 3,* 486–498.

Lack, L. C. (1978). *Selective attention and the control of binocular rivalry.* The Hague, The Netherlands: Mouton.

Leopold, D. A., & Logothetis, N. K. (1999). Multistable phenomena: changing views in perception. *Trends in Cognitive Sciences, 3,* 254–264.

Levelt, W. J. M. (1967). Note on the distribution of dominance times in binocular rivalry. *British Journal of Psychology, 58,* 143–145.

Logothetis, N. K., Leopold, D. A., & Sheinberg, D. L. (1996). What is rivalling during binocular rivalry? *Nature, 380,* 621–624.

Mamassian, P., & Goutcher, R. (2005). Temporal dynamics in bistable perception. *Journal of Vision, 5,* 361–375.

McDougall, W. (1906). Physiological factors of the attention process (IV). *Mind, 15,* 329–359.

Meng, M., & Tong, F. (2004). Can attention selectively bias bistable perception? differences between binocular rivalry and ambiguous figures. *Journal of Vision, 4,* 539–551.

Meredith, G. M., & Meredith, C. G. W. (1962). Effect of instructional conditions on rate of binocular rivalry. *Perceptual and Motor Skills, 15,* 655–664.

Peterson, M. A., & Hochberg, J. (1983). Opposed-set measurement procedure: a quantitative analysis of the role of local cues and intention in form perception. *Journal of Experimental Psychology: Human perception and performance, 9,* 183–193.

Strüber, D., & Stadler, M. (1999). Differences in top-down influences on the reversal rate of different categories of reversible figures. *Perception & Psychophysics, 28,* 1185–1196.

Suzuki, S., & Peterson, M. A. (2000). Multiplicative effects of intention on the perception of bistable apparent motion. *Psychological Science, 11,* 202–208.

Suzuki, S., & Grabowecky, M. (2002). Evidence for perceptual "trapping" and adaptation in multistable binocular rivalry. *Neuron, 36,* 143–157.

Toppino, T. C. (2003). Reversible-figure perception: mechanisms of intentional control. *Perception & Psychophysics, 65,* 1285–1295.

van Dam, L. C. J., & van Ee, R. (2005). The role of (micro) saccades and blinks in perceptual bi-stability from slant rivalry. *Vision Research, 45,* 2417–2435.

van Dam, L. C. J., & van Ee, R. (2006). The role of saccades in exerting voluntary control in perceptual and binocular rivalry. *Vision Research, 46,* 787–799.

van den Berg, A. V., & van Loon, E. M. (2005). An invariant for timing of saccades during visual search. *Vision Research, 45,* 1543–1555.

van Ee, R. (2005). Dynamics of perceptual bi-stability for stereoscopic slant rivalry and a comparison with grating, house-face, and Necker cube rivalry. *Vision Research, 45,* 29–40. doi:10.1016/j.visres.2004.07.039.

van Ee, R., van Dam, L. C. J., & Brouwer, G. J. (2005). Voluntary control and the dynamics of perceptual bi-stability. *Vision Research, 45,* 41–55. doi:10.1016/j.visres.2004.07.030.

Walker, P. (1978). Binocular rivalry: central or peripheral selective processes? *Psychological Bulletin, 85,* 376–389.

Washburn, M., & Gillette, A. (1933). Studies from the Psychological Laboratory of Vassar College: LXII. Motor factors in voluntary control of cube perspective fluctuations and retinal rivalry fluctuations. *American Journal of Psychology, 45,* 315–319.